

ENERGY STORAGE TECHNOLOGIES BASED ON ELECTROCHEMICAL DOUBLE LAYER CAPACITORS: A REVIEW

Y. A. Maletin,^{1,2} N. G. Stryzhakova,^{1,2} S. O. Zelinskyi,^{1,2}
and S. I. Chernukhin^{1,2}

UDC 544.636

Modern design approaches to electric energy storage devices based on nanostructured electrode materials, in particular, electrochemical double layer capacitors (supercapacitors) and their hybrids with Li-ion batteries, are considered. It is shown that hybridization of both positive and negative electrodes and also an electrolyte increases energy density of an electrochemical system, thus, filling the gap between supercapacitors and batteries in terms of specific energy and power, as well as charge rate and the number of charge-discharge cycles.

Keywords: supercapacitors, pseudocapacitors, “capacitor-battery” hybrids, nanostructured electrodes.

INTRODUCTION

Batteries of different types are the most well-known, deeply studied, and widely used among storage devices and electrical energy sources based on electrochemical systems. Charge-discharge processes in batteries involve reversible electrochemical transformations in the volume of two electrode materials, selected in such a way that these processes occur in negative and positive potential ranges that are the most distant from each other. The potential difference of electrodes determines the operating voltage range of a particular type of battery. This difference tends to be increased, since the energy stored and given by a battery is proportional to its voltage. Lithium-ion batteries can serve as an example [1, 2], in which the charging process is performed by input or intercalation of lithium ions into anode material (usually graphite or lithium titanate) with simultaneous output/deintercalation of lithium ions from cathode material. A relatively wide range of mixed valence lithiated metal oxides or phosphates can be used as such a material. The reverse process occurs during discharge, in particular, deintercalation of lithium ions from the anode material and their intercalation into the cathode material. The maximum operating voltage of charge usually reaches 4.3 V, while the minimum voltage is not recommended to be lower than 2.5 V during discharge. Solutions of chemically stable lithium salts, such as tetrafluoroborate, hexafluorophosphate, or lithium bis(trifluoromethanesulfonyl)imide in carbonate solvents, such as a mixture of ethylene carbonate and methyl ethyl carbonate, are used as electrolytes and solid state systems have also been developed recently. The specific energy of commercially available lithium-ion batteries reaches 350-750 kJ/kg (depending on the requirements for specific power) with a number of charge-discharge cycles of up to 3000 and, in some cases, up to 5000 cycles. These figures significantly exceed the

¹Institute for Sorption and Problems of Endoecology, NAS of Ukraine, Kyiv, Ukraine. E-mail: ymaletin@gmail.com.

²Ltd. “YUNASKO” Ukraine, Kyiv, Ukraine.

characteristics of “veterans” of the battery industry, in particular, lead-acid batteries with an energy of 120-150 kJ/kg and a number of deep charge-discharge cycles of about 400-500. Nowadays, lithium-ion batteries dominate in consumer electronics and the electric car industry; at the same time in 2019 the Nobel Prize in Chemistry was awarded for their development.

Electric double layer capacitors are fundamentally different types of electrical energy storage devices [3-5], which are also known as supercapacitors (SC), ultracapacitors or (obsolete name) liquid ionistors. Nanostructured carbon materials, such as specially synthesized activated carbon, carbon nanotubes, or graphene, are most commonly used in electrodes of these systems. There is no difference in potentials between electrodes, and there is no possibility to generate electricity since the electrodes are made of the same material, soon after producing an electrochemical cell from two such electrodes, separated by a porous dielectric separator and impregnated with electrolyte. The accumulation of energy occurs due to the application of a potential difference to the electrodes from an external source, which leads to the separation of charges in the electrolyte and the formation of an electric double layer (capacitor) on each electrode. The plates of these capacitors include negatively charged ions on the positive electrode of the electrolyte side and the positively charged ions on the negative electrode. The corresponding charges of opposite sign are plates on the sides of the electrodes, which are generated in a conductive matrix of the electrode material [6]. The simplest equivalent circuit of the obtained system can be represented as two capacitors connected in series through the resistance of the electrolyte, while the total capacity (C_{total}) of such a system is described by the equation

$$C_{\text{total}} = \frac{C_+ C_-}{C_+ + C_-}, \quad (1)$$

where C_+ and C_- are the capacitance of the electric double layer on the positive and negative electrodes. This equation will help to further understand some properties of SC design and its hybrid systems with batteries.

The SC operating voltage reaches 2.5-3.0 V in the case of organic aprotic electrolytes. The specific energy of SC does not exceed 20-30 kJ/kg, since only the electrode surface is involved in energy storage rather than its entire volume in this case; at the same time, the typical value is 15-25 kJ/kg for commercially available products, which is significantly lower when compared to all types of industrial batteries. However, on the other hand, the absence of delayed solid-phase diffusion (for example, intercalation and deintercalation of lithium ions) in the structure of the electrode material and the participation of only rapid ion diffusion in the electrolyte volume in the SC charge-discharge processes leads to a significant decrease in internal SC resistance when compared to battery systems, as well as reduction of the degradation level of electrodes during continuous cycling. The SC advantages over batteries include higher specific power at high values of energy conversion efficiency, fast charging, and continuous cycling (up to a million charge-discharge cycles).

Modern SC technology and ways of increasing its specific energy are discussed below.

CURRENT THEORY AND TECHNOLOGY OF SUPERCAPACITORS

Activated carbon materials are used as a material of electrodes in the vast majority of modern SC, the pore size of which does not normally exceeds 5 nm; according to our data, the optimal pore size is 1-3 nm. Although narrower pores can increase electrostatic capacitance [7], they significantly slow down electrolyte diffusion in the electrode porous structure. On the other hand, mesoporous materials are characterized by a smaller specific surface area and, as a result, a smaller capacitance. The presence of pores of different sizes and shapes in the electrode material and, accordingly, their different availability for electrolyte, is manifested in the fact that charge-discharge curves and SC impedance spectra, as a rule, cannot be described by a single RC circuit. A model of distributed RC-circuits of De Levie is widely used for such porous electrodes [8, 9], which provides an infinite number of such circuits; however, in most cases a good correlation of experimental and calculated data is achieved by using a circuit of two links, as shown in Fig. 1. This correlation was obtained both for the discharge curves at different loads [10, 11] and in the description of the impedance spectra [12]. A satisfactory correlation was observed [12] for SC with the highest power when the spectrum was modeled using only one RC- circuit.

This review does not contain a detailed description of the impedance spectra since some authors have recently submitted a detailed article on this topic. It should be noted that SC containing carbon electrode materials with a relatively

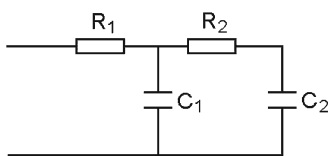


Fig. 1. Equivalent model of two RC-chains, which provides a good description of SC charge-discharge processes.

narrow pore size distribution and a low internal resistance show spectra that are close to theoretical, with a dominant capacitive component in the low frequency range. The contribution of an induction component is insignificant in the vast majority of SC with different design solutions.

There were multiple attempts to provide a complete theoretical description of the charge-discharge processes of SC electrodes involving various models of their structure aimed at finding the optimal porous structure, electrode thickness, etc. (see, for example, [13, 14]). Unfortunately, these attempts were not successful; therefore, the electrode characteristics should be considered together with the electrolyte characteristics [15, 16]; at the same time, stationary models do not consider possible changes in electrolyte mobility in pores of different sizes. The possible quantitative effect of such a change on the SC characteristics was first shown by Kalugin et al. [17]; calculations within molecular dynamics showed a significant slowdown in the diffusion of acetonitrile in carbon nanotubes with a decrease in their diameter, which was caused by the increasing effect of confinement. Since acetonitrile is the most common solvent in SC technology, it is necessary to perform experimental tests of mobility reduction of its electrolytes in nanoporous activated carbon materials, which are widely used in SC electrodes.

It should be noted that analysis of all possible contributions to the SC internal resistance shows [5] that a decrease (about 70%) in electrical conductivity of an electrolyte is dominant in the nanoporous structure of an electrode. Piezoquartz microweighing and NMR measurements *in situ* experimentally showed an accumulation of electrolyte ions with a charge opposite to the sign of applied potential; at the same time, electrolyte ions can be partially desolvated when potentials are applied to SC electrodes in nanopores of electrode materials [18]. The NMR method of pulsed field gradient stimulated spin-echo was chosen [19] to determine the mobility of electrolyte ions in such nanopores, which is widely used to measure diffusion coefficients in liquids [20]. The work [19] used this method and an attachment for spin-echo measurements in solids to study the electrolyte diffusion processes in nanopores of activated carbon powders. The NMR ampoule contained common SC components, such as powder of nanoporous carbon material impregnated with a solution of ethyltrimethylammonium tetrafluoroborate ($\text{EtMe}_3\text{N}^+\text{BF}_4^-$)* in acetonitrile. Measurements were performed on ^1H and ^{19}F nuclei, providing a satisfactory correlation of the obtained values of diffusion coefficients with the change in the internal resistance of SC prototypes using the same powders as electrodes.

The diffusion coefficients were also determined by cyclic voltammetry with a rotating disk electrode [21], on which a layer of nanoporous carbon powder was deposited in order to further verify the results of these measurements. The measurements with a porous rotating electrode also showed [19] a satisfactory correlation between ion diffusion slowdown in nanopores of different carbon materials and an increase in the resistance of SC prototypes in which these materials were used as electrodes.

It should be noted that the obtained values of diffusion coefficients for the eight studied nanoporous carbon materials [19] differ significantly for BF_4^- anion (from $5 \cdot 10^{-10} \text{ m}^2 \cdot \text{s}^{-1}$ to $14 \cdot 10^{-10} \text{ m}^2 \cdot \text{s}^{-1}$) and for EtMe_3N^+ cation (from $1.25 \cdot 10^{-10} \text{ m}^2 \cdot \text{s}^{-1}$ to $2.05 \cdot 10^{-10} \text{ m}^2 \cdot \text{s}^{-1}$). Although the values of diffusion coefficients obtained using both methods are obviously average values for pores of different sizes, it is not surprising that the diffusion coefficient values and the corresponding SC resistance are

*Tetrafluoroborate tetraethylammonium is also often used. The electrical conductivity of such electrolytes in acetonitrile reaches 55-60 mS/cm at room temperature.

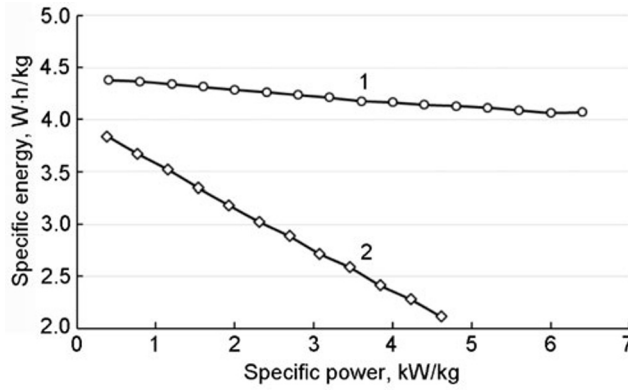


Fig. 2. Dependence of available energy on the amount of load for SC with the same capacity of 1400 F but with different internal resistance: 0.09 mΩ (1) and 0.50 mΩ (2).

correlated when considering the De Levie model and its simplified representation in Fig. 1, which also summarizes the resistance of different RC-circuits. According to the obtained data, the measurement method for effective diffusion coefficients was patented [22] to select materials for positive and negative SC electrodes with the lowest internal resistance and, accordingly, the highest values of specific power and efficiency.

It should also be noted that low internal resistance, even though it does not determine the maximum SC energy stored (Eq. (3)), significantly affects the dependence of available energy on the amount of load. Figure 2 shows results [23] of studies of the SC samples produced by different manufacturers with the same capacity values (about 1400 F) and operating voltage (2.7 V) but with significant difference in internal resistance. Figure 2 shows how low resistance stabilizes high energy level when load is increased. The use of SC is usually associated with high loads, and in these cases, low resistance can double useful energy and, as a result, significantly reduce the level of energy dissipation in the form of heat, in particular, power source heating. It is possible to avoid dangerous power supply overheating in many cases and eliminate its active cooling when using SC with low internal resistance.

In addition to low internal resistance, the SC operating voltage is another important factor involved in specific power and specific energy increase. The maximum values of power (P_{\max}) and energy (E_{\max}) are proportional to the square of the voltage:

$$P_{\max} = \frac{U^2}{4R_{\text{in}}}, \quad (2)$$

$$E_{\max} = \frac{CU^2}{2}, \quad (3)$$

where U is the SC operating voltage; C is the capacitance; R_{in} is the internal resistance. The operating voltage of commercially available SC is in the range of 2.5-3.0 V with tetraalkylammonium tetrafluoroborate solutions in acetonitrile, which are used as electrolytes. Cyclic voltammetry (CV) is used to select electrode materials that can provide high SC operating voltage, as shown in [19]; examples are shown in Figs. 3 and 4.

It is possible to increase the SC operating voltage to 3.0 V or even higher by increasing self-discharge and reducing lifetime by means of different carbon materials for positive and negative electrodes.

It is almost impossible to increase the operating voltage by using other aprotic solvents instead of acetonitrile. For example, the work [24] showed that acetonitrile limits the growth of the positive electrode potential, while the use of propylene carbonate limits the range of negative potentials. The use of ionic liquids has not solved the problem yet, as their high

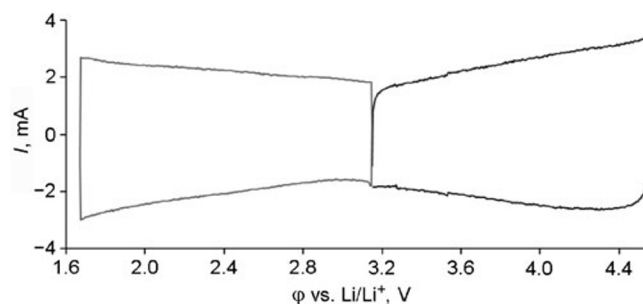


Fig. 3. For example, CV for a three-electrode cell with a potential sweep of working electrode in the positive and negative regions of its equilibrium potential (potentials are relative to lithium potential, which is 0 V).

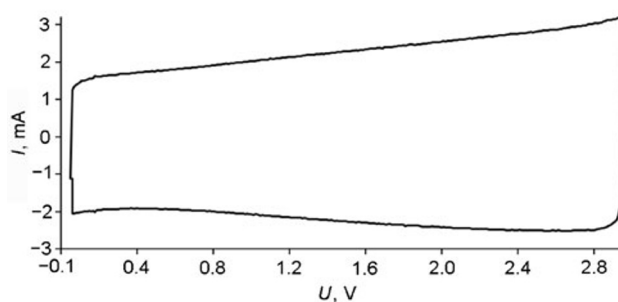


Fig. 4. An example of CV in a SC model with electrodes selected for the positive and negative potential regions according to the method shown in Fig. 3.

electrochemical resistance is neutralized by their high viscosity at room temperature and, consequently, low electrical conductivity. The increase in electrical conductivity by increasing temperature is accompanied by a significant decrease in their electrochemical stability (“electrochemical window” narrowing) (see, for example, Table 1 and comments). Their limited use in SC technology, which mainly involves high-temperature applications, is due to the higher cost of ionic liquids when compared to known aprotic electrolytes [25].

It should be noted that SC operating temperature increase can be achieved not only by ionic liquids but also by some organic solvents with boiling points around 200°C, such as benzonitrile, which enable operation of the SC at a temperature of 100°C and above [26], and which show even better performance when compared to ionic liquids. For example, the characteristics of SC from the FastCap Co., USA [25], one of the leaders in the use of ionic liquids (IL) and vertically oriented carbon nanotubes in the electrode, can be compared with the SC characteristics based on benzonitrile (PhCN) and nanoporous activated carbon[†] [26] (Table 1).

Table 1 shows the low operating voltage of SC with ionic liquid at 100°C (while the voltage drops to 1.5 and 1.0 V at 125°C and at 150°C respectively [25]). The internal resistance of SC with ionic liquid remains quite high even at 100°C; which is shown by the comparison of RC constants: 2.7 s and 0.66 s for SC with ionic liquid and 0.20 s for SC with benzonitrile. The RC constant value determines the SC charge-discharge rate, for example, the degree of charge Q_t for time t is determined by

[†]The results of our tests, as well as tests performed at the JME Laboratory, Cleveland, USA.

TABLE 1. SC Characteristics Based on Ionic Liquid and Benzonitrile at 100°C

Electrolyte/solvent	Capacity, F	Resistance, mΩ	Voltage, V	Weight, kg	Specific energy, kJ/kg
IL [25]	370	7.4	2.0	0.11	6.7
IL [25]	38	17.3	2.0	0.021	3.6
PhCN [26]	200	1.0	2.5	0.052	12.0

$$Q_t = Q_f \left(1 - e^{-\frac{t}{RC}} \right), \quad (4)$$

where Q_f is the full charge of the SC.

The relatively low specific energy of the first two SCs in Table 1 is obviously due to the inaccessibility of a significant part of the nanotube surface for a viscous electrolyte, as well as the low operating voltage.

Recently, their modification by nitrogen heteroatoms is often used to improve the performance of SC electrode materials [27]. The surface of nanoporous carbon can be effectively modified as a result of, for example, thermal decomposition of melamine with the release of ammonia [28, 29]. The work [28] shows that pre-oxidation of activated carbon allows one to introduce an increased (compared to unoxidized) and adjustable amount of nitrogen into its surface. Surface oxidation methods are well known [30] and, according to our observations, oxidation with subsequent nitrogen modification allows one to reduce the SC internal resistance and increase its operating voltage and specific power in some cases [29]. This method can be especially promising when using microwave treatment, the duration of which does not exceed 8-10 min, instead of continuous and energy-consuming treatment of a mixture of carbon material with melamine in a tubular furnace [31].

When new allotropic modifications of carbon, such as carbon nanotubes and graphene, were discovered, researchers have tried to use them in SC electrode materials for several years [32, 33]. However, despite numerous assumptions of high performance of these materials, there was no practical evidence of such a fact in real prototypes or commercial samples of SC. For example, Table shows the SC technical characteristics of the FastCap Co. [25] with electrodes containing vertically oriented nanotubes on a current collector. Their use (in this case in combination with ionic liquids) does not provide any advantages over nanoporous activated carbon materials. Similar results were obtained in our laboratory with nanotubes from other manufacturers; in particular, SC prototypes with electrodes based on nanotubes or commercially available nanoporous activated carbon produced under the same conditions showed significantly higher parameters in the second case. This may be due to the availability constraints of the inner surface of nanotubes, as discussed above and in [17, 19], as well as the low specific value of their outer surface.

Attempts to replace nanoporous activated carbon in SC electrodes with graphene led to a decrease in performance in some cases [34]. Thus, the four studied samples of graphene had the following values of specific surface area (DFT) and electrostatic capacitance: 1440 m²/g and 84 F/g, while the corresponding values of the best commercially available nanoporous carbon materials obtained from coconut shells are in the range of 2100-2400 m²/g and 112-130 F/g [34]. The significant reduction in specific surface area (and, consequently, capacity) may be caused by a partial aggregation of single-layer graphene fragments into multilayer ones. On the other hand, the Graphene Energy Co., USA, reported [35] the development of laboratory samples of SC based on graphene and ionic liquid with an operating voltage of 3.5 V and energy stored of about 70 kJ/kg. However, the subsequent works involving the same Ruoff's team show [36, 37] that in this case the electrode material was obtained by chemical activation of thermally expanded graphite with potassium hydroxide. The material has a three-dimensional structure with pores ranging in size from 0.6 to 4 nm, with high specific surface area and capacity of about

150 F/g. Therefore, the properties of the obtained material are obviously associated with three-dimensional activated carbon, which is not subject to aggregation, rather than with single-layer graphene. The aggregation of single-layer graphene was prevented in the works of Miller et al. [38, 39] through the production of ultra-thin electrodes (0.6 μm) using vertically oriented graphene petals on a metal substrate. At the same time, obtaining an energy-intensive system was not the goal; rather, the possibility of replacing aluminum electrolytic capacitors with RC constant at the level of 0.1 ms for current filtration circuits at a frequency of up to 120 Hz was studied. An effective increase in SC energy density can be achieved by creating so-called pseudocapacitors or hybrid systems that include components of SC and batteries.

PSEUDOCAPACITORS (PC)

The name “pseudocapacitors” involves electrochemical systems in which the capacity of the electric double layer is supplemented by the electrode-electrolyte distribution surface by charge transfer processes across this boundary [3, 40, 41]. Since the charge accumulation process involves both the surface and volume of the electrode, PCs show almost twice the specific energy when compared to common SCs. The first PC samples included Ru and Ir hydrated oxides as an active electrode material, although there were attempts to use oxides of other transition metals [42, 43]. The redox transition $\text{Ru}^{\text{III}}/\text{Ru}^{\text{IV}}$ is associated with rapid proton exchange between oxide and hydroxide sites. High capacity (up to 500 F/g based on active mass) and high values of velocity/current were obtained for the charge-discharge processes due to reversible reactions on the electrode surface. However, these systems have not been widely used due to low availability and high cost of the most efficient Ru and Ir-based materials.

Over the last two decades, polymers with high electronic conductivity, such as polyaniline, polypyrrole, and polythiophene have also been studied as PC electrodes [44-46]. The Crosslink Co., USA showed [46] the characteristics of PC button cells with polyaniline-based electrodes with a specific power of several kW/kg (depending on design) and an energy of about 20 kJ/kg taking into account the weight of the polymer, which is comparable to the characteristics of existing SCs. On the other hand, Barsukov et al. [44, 45] proposed a “capacitor” concept with polyaniline-based electrode with the possibility of obtaining ultra-high specific capacity (up to 500-600 F/g). However, these studies reported the gradual formation of a nonconductive layer in polyaniline near the boundary of the current collector. Developers of PC based on electrically conductive polymers are faced with this effect, which may be at least one of the reasons for rapid degradation of the system and reduction in the number of charge-discharge cycles, thus preventing their entry into the energy storage market.

Recently, the group of Gogotsi and Barsoum [47, 48] synthesized a new class of materials under the general name MXene, in particular, two-dimensional carbides or nitrides of transition metals. The resulting materials, such as Ti_3C_2 , form a layered structure with a layer thickness equal to several atoms. The material has high electronic conductivity; at the same time, the intercalation of various ions into an interlayer space is possible. Various possible applications of MXenes are offered, in particular, as electrode materials for PC with high specific capacity; however, these concepts have not gone beyond laboratory studies yet. Nevertheless, it is important to obtain data on resource tests of these promising materials, PC behavior based on them in a wide temperature range, and capacity dependence on current, etc.

Another type of material that can be classified as PC is based on metal complexes with organic ligands. There are known attempts at using complex compounds in the polymer matrix as electrode materials, such as complexes of mixed valence metals with Schiff bases derived from salicylic aldehyde and aliphatic diamines [49], which can be reversibly oxidized and reduced in the desired potential range. The use of such metal complexes has not gone beyond laboratory studies yet, which is due to the insufficient reversibility of their redox transformations and insufficiently high capacity at a relatively high cost. Recently, metal-organic framework structures (MOF) have gained popularity, which are considered a new class of porous materials with a high specific surface area and a large volume of pores [50, 51]. However, the direct application of MOF in PC is still limited by their low electrical conductivity and insufficient electrochemical resistance. On the other hand, MOF-based framework structures contain more carbon and may be used as precursors for the template synthesis of nanoporous carbon materials with a given pore structure and transport channels. The study [51] showed one of the first examples of such template synthesis of nanoporous carbon material with a high specific surface area and good electrode characteristics when used in PC, in which an MOF-5 framework structure ($\text{Zn}_4\text{O}(\text{OOC}_6\text{H}_4\text{COO})_3$) with a three-dimensional intersecting channel system and a cavity diameter of 1.8 nm and furfuryl alcohol was used as a precursor. The obtained electrode material showed a maximum

specific capacitance of 312 F/g. This template synthesis in combination with doping by nitrogen heteroatoms contributes to the production of electrode materials with a specific capacitance of 270 F/g, regardless of cycling with a current of 2 A/g [50]. In addition, MOFs contribute to the production of composite materials containing nanoparticles of metal oxides, such as CoO/Co₃O₄ [52], thus increasing the capacitance of the system by adding pseudocapacitance by means of redox processes involving these nanoparticles. Further studies of MOF in SC and PC systems appears promising.

COMBINED AND HYBRID SC SYSTEMS WITH BATTERIES

According to the above data, a significant increase in SC energy density due to the use of new carbon materials in electrodes and/or new electrolytes seems unlikely. Pseudocapacitor systems have not provided a significant breakthrough yet. Therefore, the technology of storage and power sources until recently proceeds in two directions: in one, the SC is used to obtain short-term superpower energy pulses and, in the other hand, (mainly) LIB is used to provide high specific energy at low specific power. If the former “suffers” from a lack of energy, the use of the latter can be dangerous in high power modes, especially during fast charging involving high current. There are numerous well-known cases of their uncontrolled overheating, destruction, and even combustion that are caused mainly by such modes [53]. A combination of SC and LIB could be a natural solution to this issue, in particular, parallel connection of two power supplies, where LIB provides the required energy consumption, while SC covers peak loads. Such a module with a voltage of 12 V was implemented by us; indeed, the SC fragment successfully withstood peak loads, allowing the LIB fragment to operate in an energy-saving mode and maintain the SC fragment voltage (see Fig. 5).

However, the parallel combination of two current sources, each of which consists of series-connected elements of SC and LIB aimed at achieving the desired voltage, leads to a corresponding increase in mass and volume caused by a separate packaging of each source, two control and monitoring systems (BMS), and additional contacts. This increase may be insignificant for a number of stationary applications, but the weight and/or volume of power supply is very critical for numerous moving or portable objects, such as aircrafts, cars, and smart phones. Therefore, other solutions should be sought, one of which may involve internal hybridization of electrochemical systems of SC and batteries at the level of electrode materials and electrolytes. Theoretical principles of such hybridization were formulated in the known studies [3, 4, 54]. In addition, some examples of practical implementation of hybrid systems will be considered below.

According to the terminology [54], the principle of asymmetric or “serial” connection of electrodes using SC and battery technology was implemented in the first hybrid systems. For example, the first industrial hybrid [55, 56] included nanoporous carbon material (SC fragment) in the negative electrode and nickel hydroxide (technology of nickel-cadmium or nickel-metal hydride batteries) in the positive electrode. This hybrid system doubled the energy density of the SC, providing fast charging within 15 min using inexpensive electrode elements and an aqueous alkaline electrolyte. It is not surprising that the technology was licensed by SAFT to power large diesel vehicles [57]. It is assumed that the use of a hybrid capacitor will optimize battery performance and provide the necessary power to start diesel engines even at low temperatures or for frequent starts in a start-stop system.

Later, similar serial hybrids were developed [58, 59] using a positive electrode and an electrolyte involving technology of lead-sulfuric acid batteries; at the same time, nanoporous carbon material was used in the negative electrode. The advantages of the system included low-cost elements, well-designed technology for the production of lead-sulfuric acid batteries, and a twofold increase in specific energy when compared to common SC.

Serial hybridization of SC with LIB has also been successfully performed. This type of hybrids is known as LIC (Li-ion capacitor) [60-64]. As for battery technology, LIC usually includes an anode, most often graphite, although turbostratic carbon (“hard carbon” in the English literature) [62] or lithium titanate, Li₄Ti₅O₁₂ [64], was used in some cases. An original approach was proposed using a composite material such as nanoparticles of lithium titanate deposited on carbon nanofibers [65, 66]. The industrial development of LIC was carried out by the JSR Micro Co. [60, 63]. Hybrid capacitors and modules with an operating voltage of up to 45.6 V and a capacity of up to 800 F, produced under the brand of ULTIMO, show high discharge currents and a large number of charge-discharge cycles.

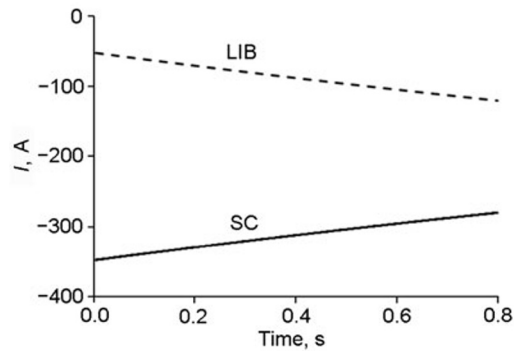


Fig. 5. Distribution of current between SC and LIB fragments when discharging the combination module with a voltage of 12 V. Total discharge current $I = 400$ A, module mass 2.2 kg.

It should be noted, however, that all of the above technologies of asymmetric or serial hybridization can only double the capacity of common SCs. According to Eq. (1) the total system capacity is limited to the significantly lower capacity electrode of SC technology in this case, where only the capacity of the electric double layer is realized. Although higher values were obtained for laboratory samples, ULTIMO modules have specific energy only in the range of 40-50 kJ/kg [62]. On the other hand, Eq. (1) suggests a way of overcoming this limitation. It is not enough to increase the capacity of only one electrode, but it is necessary to find a way to increase the capacity of both positive and negative electrodes.

The theoretical justification of such a symmetric solution was proposed in the study of Kotz et al. [54], which is called a “parallel” hybrid. It was implemented in practice in our works [67, 68]. The system proposed by us has the following properties.

- Both positive and negative electrodes are obtained by mixing powders of nanoporous carbon material and lithium transition metal oxide or phosphate; the negative electrode contains nanosized lithium titanate powder, while the positive electrode contains any cathode material known in the technology of Li-ion batteries. According to Figs. 3 and 4, nanoporous carbon in the positive and negative electrodes can be different, aimed at better matching of potential ranges with battery components. In general, the active components of the obtained composite electrodes should be carefully matched to the mass and ranges of the operating potentials, thus preventing the allowable potential intervals in the charge-discharge processes to be exceeded.

- A binding agent and electrically conductive additive (special carbon black and/or graphite) are added to the powder mixture of the active electrode components; the resulting composite is deposited on aluminum foil (current collector), thus forming an electrode.

- It is desirable to use solutions of chemically stable lithium salts as an electrolyte, which are common for Li-ion battery technology, such as lithium *bis*(trifluoromethanesulfonyl)imide (LiTFSI) in acetonitrile. It is necessary to use acetonitrile instead of carbonate solvents, which are commonly used in the technology of Li-ion batteries, to increase electrical conductivity. It is also possible to add tetraalkylammonium salts to the electrolyte for this purpose.

As a result, such hybridization of the entire electrochemical system (both electrodes and electrolyte) leads to a significant increase in specific energy; in particular, energy density of the first generation parallel or symmetrical hybrids was raised to 120-130 kJ/kg [5]. Currently, the second generation of such hybrids shows energy density of up to 220 kJ/kg while maintaining the inherent high discharge currents for SC, possibility of fast charging, and continuous cycling. Some of the important characteristics for practical use are shown in Figs. 6 and 7.

Figure 6 shows the charge-discharge curves of a parallel hybrid manufactured by Yunasko-Ukraine. The figure shows the two main distinguishing characteristics of the hybrid system when compared to its “parents,” such as SC and LIB. In contrast to SC, the charge and discharge curves of the hybrid system to relatively high currents (order of 10C) are characterized by a flat plateau in the region above 2 V, apart from an order of magnitude higher specific energy. The SC charge and discharge

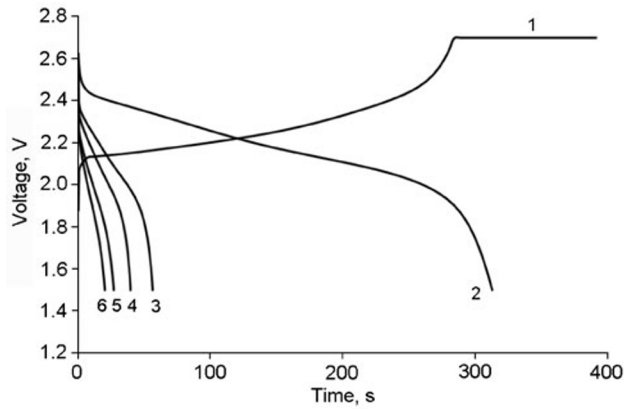


Fig. 6. Charge-discharge curves of the hybrid sample with a capacity of 3 A·h and a mass of 110 g in galvanostatic mode: 1) charge with a current of 30 A; 2) discharge with a current of 30 A; 3) discharge with a current of 150 A; 4) discharge with a current 200 A; 5) discharge with a current 250 A; 6) discharge with a current of 300 A.

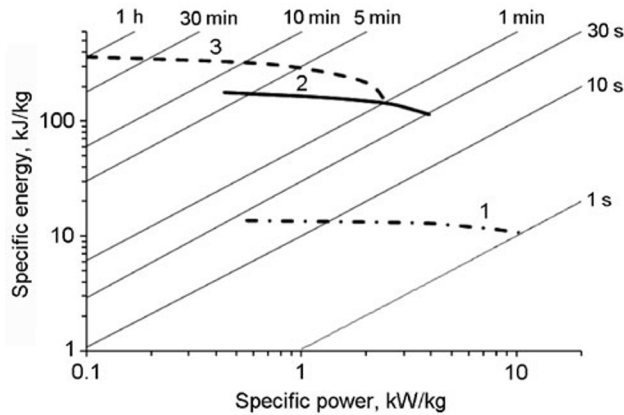


Fig. 7. Ragone plots: 1) SC; 2) the hybrid sample of Yunasko-Ukraine company; 3) a common high-power Li-ion battery [71].

in the galvanostatic mode is accompanied by a linear change in voltage, which requires an additional connection of a dc-dc converter for many practical applications. The ability to discharge by large current (for example, 300 A for 20 s for a sample weighing only 110 g (Fig. 6, curve 6) and the possibility of a full charge in just 5-6 min is an important difference when compared to LIB. An additional advantage of the hybrid system over LIB is a significant increase in the number of charge-discharge cycles: 3,000 complete cycles is the default value for LIB, while the hybrid system can operate steadily for up to 30,000 or even more cycles.

Visual comparison of the characteristics of different electrical energy sources is usually performed by Ragone plots [69, 70]. The dependence of specific energy on specific power of discharge is built into the logarithmic scale, which is delivered to a load. Figure 7 shows plots for the SC samples (curve 1), high-power version of LIB [71] (curve 3), and hybrid sample (curve 2), the charge-discharge curves for which are presented in Fig. 6. All three curves indicate a decrease in useful energy when load is increased, which is similar to Fig. 2 for SC with different internal resistance. This effect is caused by the dissipation of energy partially in the form of Joule heat, which is released inside the current source and the value of which is

proportional to its internal resistance. Such dissipation is highly undesirable not only due to the partial loss of energy, but it can also pose the risk of uncontrolled overheating of the source, which has already led to the combustion of LIB in some cases [53].

Figure 7 also shows a characteristic time grid [69] for different current sources, indicating which part of energy can be obtained at full discharge at a given period of time. Figure 7 shows that the use of SC can provide high specific power (10 kW/kg and even higher), but for a short period of time, in particular, less than 20 s and up to a sub-second range, which can be effectively used, for example, for sharp acceleration of electric cars [23], in start-stop systems in hybrid cars (for example, in Peugeot e-HDi), and in portable welding equipment [72]. Common LIBs with a specific energy of about 700 kJ/kg have slow charging and discharging process and are not shown in Fig. 7. Nevertheless, the characteristic discharge time should be chosen between 5-10 min or above even for high-power LIB to avoid a high level of energy dissipation into heat. The niche between the high-power LIB and SC is successfully filled by hybrid systems, which can be discharged quite effectively in the period from 20 s to 10 min and which can also be fully charged in 5-6 min.

CONCLUSIONS

1. Currently, supercapacitors are the best candidates for high specific power devices. They are able to provide discharge pulses in the range of 10-50 kW/kg, the possibility of a full charge in seconds, and almost unlimited cycling. However, they are competitive only in the time interval from milliseconds to 10 s due to the relatively low energy density.

2. Pseudocapacitor systems and supercapacitor hybrids with different types of batteries, in which one of the electrodes belongs to supercapacitor technology, are able to double their specific energy, which is enough to expand their applications.

3. Combined systems in which a supercapacitor is connected in parallel to a battery and can effectively cover peak loads, thus allowing the battery to operate safely and for longer periods of time, have limited use except in a number of cases.

4. Hybrid systems, in which the combination of supercapacitor elements and lithium-ion batteries is carried out at the level of a single electrochemical system, are able to increase the energy density of supercapacitors while maintaining higher specific power and a larger number of charge-discharge cycles when compared to batteries, as well as provide a full charge in just 5 min.

ACKNOWLEDGEMENT

The work was performed with the financial support of the target research program of the NAS of Ukraine “New functional substances and materials of chemical production” (projects №0117U000860, 0119U000619) and the target comprehensive interdisciplinary research program of the NAS of Ukraine on sustainable development and environmental management in global environmental change (projects No. 0115U002963, 0119U000719, 0120U103052).

REFERENCES

1. J. B. Goodenough and K. S. Park, *J. Am. Chem. Soc.*, **135**, No. 4, 1167-1176 (2013), doi: 10.1021/ja3091438.
2. S. A. Kirillov, *Theor. Exp. Chem.*, **55**, No. 2, 73-95 (2019), doi: 10.1007/s11237-019-09598-2.
3. B. E. Conway, *Electrochemical Supercapacitors: Scientific Fundamentals and Technological Applications*, Kluwer-Plenum Press, New-York (1999).
4. F. BeMguin and E. Frackowiak, *Supercapacitors: Materials, Systems, and Applications*, Wiley-VCH, Weinheim (2013).
5. Yu. A. Maletin, H. G. Strizhakova, C. A. Zelinsky, et al., *Ukr Khim. Zh.*, **83**, No. 11, 38-49 (2017).
6. M. A. Vorotyntsev and A. A. Kornyshev, *Electrostatics of Media with Spatial Dispersion* [in Russian], Nauka, Moscow (1993).
7. J. Chmiola, G. Yushin, Y. Gogotsi, et al., *Science*, **313**, 1760-1763 (2006), doi: 10.1126/science/1132195.
8. R. De Levie, *Adv. Electrochem. Electrochem. Eng.*, **6**, 329-397 (1967).

9. M. Yaniv and A. Soffer, *J. Electrochem. Soc.*, **123**, 506-511 (1976).
10. Y. A. Maletin, N. G. Strizhakova, V. Y. Izotov, et al., *New Promising Electrochemical Systems for Rechargeable Batteries*, Kluwer Acad. Publ., (1996), pp. 363-372.
11. J. R. Miller, *J. Power Sources*, **326**, 726-735 (2016), doi:10.1016/j.jpowsour.2016.04.020.
12. J. R. Miller and S. M. Butler, *Electrochim. Acta.*, **305**, 1-9 (2019), doi:10.1016/j.electacta.2019.03.021.
13. V. Yu. Izotov, D. G. Gromadskyi, and Yu. A. Malyetin, *Nauk. Visti NTUU "KPI"*, No. 6(62), 114-118 (2008).
14. X. Liu, X. Dai, G. Wei, et al., *Sci. Rep.*, **7**, 45934 (2017), doi: 10.1038/srep45934.
15. Y. Maletin, P. Novak, E. Shembel, et al., *Appl. Phys. A*, **82**, No. 4, 653-657 (2006), doi:10.1007/s00339-005-3416-9.
16. F. Beguin, V. Presser, A. Balducci, and E. Frackowiak, *Adv. Mater.*, **26**, No. 14, 2219-2251 (2014), doi:10.1002/adma.201304137.
17. O. N. Kalugin, V. V. Chaban, V. V. Loskutov, and O. V. Prezhdo, *Nano Lett.*, **8**, 2126-2130 (2008), doi: 10.1021/nl072976g.
18. J. M. Griffin, A. C. Forse, W.-Y. Tsai, et al., *Nat. Mater.*, **14**, 812-819 (2015), doi: 10.1038/nmat4318.
19. Y. Maletin, V. Strelko, N. Stryzhakova, et al., *Energ. Environ. Res.*, **3**, No. 2, 156-165 (2013), doi: 10.5539/eer.v3n2p156.
20. Y. Cohen, L. Avram, and L. Frish, *Angew. Chem. Int. Ed.*, **44**, No. 4, 520-554 (2005), doi: 10.1002/anie.200300637.
21. R. T. Bonnecaze, N. Mano, B. Nam, and A. Heller, *J. Electrochem. Soc.*, **154**, No. 2, F44-F47 (2007), doi: 10.1149/1.2759834.
22. Y. Maletin, N. Stryzhakova, S. Zelinskyi, et al., *Method for Selecting Nanoporous Carbon Material for Polarizable Electrode, Method of Manufacturing Such Polarizable Electrodes and Method of Manufacturing Electrochemical Double Layer Capacitor*, Patent US 9524830, Publ. Dec. 20, 2016.
23. S. Ghosh and D. Corrigan, *Directed Research Report on Performance of Commercial Supercapacitors*, AET-8996, Wayne State Univ., Detroit (2014).
24. P. W. Ruch, D. Cericola, A. Foelske, et al., *Electrochim. Acta.*, **55**, No. 7, 2352-2357 (2010), doi: 10.1016/j.electacta.2009.11.098.
25. <https://kamaka.de/wp-content/uploads/2018/02/FastCAP-2016-Technology-and-Product-Overview-v10.pdf>
26. N. Stryzhakova, S. Zelinskyi, D. Tretyakov, and Y. Maletin, *Electrolyte for an Electrochemical Double Layer Capacitor, and an Electrochemical Double Layer Capacitor Using Such*, Patent US 10157713 B2, Publ. 2018.
27. R. G. Shrestha, S. Maji, L. K. Shrestha, and K. Ariga, *Nanomaterials*, **10**, 639, 1-27 (2020), doi: 10.3390/nano10040639.
28. Yu. A. Tarasenko, S. V. Zhuravsky, I. N. Dukhno, et al., *Visn. Khark. Nat. Univ., Khim.* **19(42)**, No. 932, 129-138 (2010).
29. V. Trykhlil, V. Strelko, Yu. Maletin, et al., *Nitrogen-Doped Activated Carbon and Method for Nitrogen Doping Activated Carbon*, Patent CN 104039698, Publ. 2016.
30. I. A. Tarkovskaya, *Oxidized Coal* [in Russian], Naukova Dumka, Kiev (1981).
31. O. V. Gozhenko, V. Ye. Goba, A.O. Lysenko, et al., *Method of Surface Modification of Nanoporous Carbon for Electrodes of Capacitor of Double Electric Layer* [in Ukrainian], Patent Ukraine No. 145165, Publ. 2020.
32. L. F. Aval, M. Ghoranneviss, and G. B. Pour, *Heliyon.*, **4**, No. 11 (2018), doi: 10.1016/j.heliyon.2018.e00862.
33. Z. Lu, R. Raad, F. Safaei, et al., *Front. Mater.* (2019), doi: 10.3389/fmats.2019.00138.
34. S. O. Zelinskyi, N. G. Stryzhakova, and Yu. A. Maletin, *Nanosyst., Nanomater., Nanotechnol.*, **18**, No. 1, 1-14 (2020), doi: 10.15407/nnn.18.01.001.
35. D. Agnihotri, *Proc. 20th Intern. Seminar on Double Layer Capacitors and Hybrid Energy Storage Devices*, Deerfield Beach, FL, 233-243 (2010).
36. Y. Zhu, S. Murali, M. D. Stoller, et al., *Science*, **332**, No. 6037, 1537-154 (2011), doi: 10.1126/science.1200770.
37. W.-Y. Tsai, R. Lin, S. Murali, et al., *Nano Energy*, **2**, No. 3, 403-411 (2013), doi: 10.1016/j.nanoen.2012.11.006.
38. J. R. Miller, R. A. Outlaw, and B. C. Holloway, *Science*, **329**, 1637-1639 (2010), doi: 10.1126/science.1194372.
39. J. R. Miller, R. A. Outlaw, and S. Butler, *Proc. 22nd Intern. Seminar on Double Layer Capacitors and Hybrid Energy Storage Devices*, Deerfield Beach, FL, 142-151 (2012).

40. J. Ding, W. Hu, E. Paek, and D. Mitlin, *Chem. Rev.*, **118**, No. 14, 6457-6498 (2018), doi: 10.1021/acs.chemrev.8b00116.
41. S. Fleischmann, J. B. Mitchell, R. Wang, et al., *Chem. Rev.*, **120**, No. 14, 6738-6782 (2020), doi: 10.1021/acs.chemrev.0c00170.
42. S. Trasatti and P. Kurzweil, *Platin. Met. Rev.*, **38**, No. 2, 46-56 (1994).
43. P. Kurzweil and O. Schmid, *Proc. 6th Intern. Seminar on Double Layer Capacitors and Similar Energy Storage Devices*, Deerfield Beach, FL (1996).
44. V. Barsukov and S. Chivikov, *Electrochim. Acta*, **41**, Nos. 11-12, 1773-1779 (1996), doi: 10.1016/0013-4686(95)00494-7.
45. V. Z. Barsukov, V. G. Khomenko, S. V. Chivikov, et al., *Electrochim. Acta*, **46**, Nos. 26-27, 4083-4094 (2001), doi: 10.1016/S0013-4686(01)00715-0.
46. R. Mercado, V. H. Ebron, and M. Birschbach, *Proc. 21st Intern. Seminar on Double Layer Capacitors and Hybrid Energy Storage Devices*, Deerfield Beach, FL, 226-239 (2011).
47. M. R. Lukatskaya, O. Mashtalir, C. E. Ren, et al., *Science*, **341**, No. 6153, 1502-1505 (2013), doi: 10.1126/science.1241488.
48. A. Al-Temimy, B. Anasori, K. A. Mazzio, et al., *J. Phys. Chem. C*, **124**, No. 9, 5079-5086 (2020), doi: 10.1021/acs.jpcc.9b11766.
49. A. Timonov, S. Logvinov, I. Chepurnaya, and V. Kuznetsov, *Proc. 15th Intern. Seminar on Double Layer Capacitors and Hybrid Energy Storage Devices*, Deerfield Beach, FL, 261-275 (2005).
50. R. G. Shrestha, S. Maji, L. K. Shrestha, and K. Ariga, *Nanomaterials*, **10**, No. 639, 1-27 (2020), doi: 10.3390/nano10040639.
51. B. Liu, H. Shioyama, T. Akita, and Q. Xu, *J. Am. Chem. Soc.*, **130**, No. 16, 5390-5391 (2008).
52. F. Marpaung, T. Park, M. Kim, et al., *Nanomaterials*, **9**, No. 12, 1796 (2019), doi: 10.3390/nano9121796.
53. <https://www.thecompliancecenter.com/lithium-battery-catches-fire/>.
54. D. Cericola and R. Kotz, *Electrochim. Acta*, **72**, 1-17 (2012), doi:10.1016/j.electacta.2012.03.151.
55. A. D. Klementov, I. Varakin, S. Litvinenko, et al., *Proc. 7th Intern. Seminar on Double Layer Capacitors and Similar Energy Storage Devices*, Deerfield Beach, FL (1997).
56. A. B. Stepanov, I. N. Varakin, V. V. Menukhov, and A. D. Klementov, *Double Layer Capacitor*, Patent US 6181546, Publ. 2001.
57. <https://www.greencarcongress.com/2009/05/soft-esma-20090511.html>.
58. <https://www.axionpower.com/the-battery/>.
59. E. Buiel, *Proc. 20th Intern. Seminar on Double Layer Capacitors and Hybrid Energy Storage Devices*, Deerfield Beach, FL, 220-232 (2010).
60. <https://www.jsrmicro.be/emerging-technologies/lithium-ion-capacitor/products/ultimo-lithium-ion-capacitor-prismatic-cell>.
61. S. Tasaki, N. Ando, M. Nagai, et al., *Lithium Ion Capacitor*, Patent US 7697264, Publ. 2010.
62. W. J. Cao and J. P. Zheng, *Proc. 22nd Intern. Seminar on Double Layer Capacitors and Hybrid Energy Storage Devices*, Deerfield Beach, FL, 99-105 (2012).
63. A. Yahalom, Y. Dahan, V. Prihodko, and M. Averbukh, *IEEE Intern. Conf. on the Science of Electrical Engineering*, 2016, doi: 10.1109/ICSEE.2016.7806121.
64. G. G. Amatucci, F. Badway, A. Du Pasquier, and T. Zheng, *J. Electrochem. Soc.*, **148**, No. 8, A930 (2001), doi: 10.1149/1.1383553.
65. S. Ishimoto, N. Nishina, Y. Minato, and K. Tamamitsu, *Proc. 20th Intern. Seminar on Double Layer Capacitors and Hybrid Energy Storage Devices*, Deerfield Beach, FL, 161-172 (2010).
66. K. Naoi, S. Ishimoto, J. Miyamoto, and W. Naoi, *Energy Environ. Sci.*, **5**, 9363-9373 (2012), doi: 10.1039/C2EE21675B.
67. S. I. Chernukhin, D. O. Tretyakov, D. A. Sidorov, et al., *Materials of the X Intern. Conf. "Fundamental Problems of Energy Conversion in Lithium Electrochemical Systems," Saratov, RF, (2008)*, pp. 214-215.

68. S. Chernukhin, D. Tretyakov, and Y. Maletin, *Hybrid Electrochemical Energy Storage Device*, Patent US 2014/0085773 A1, Publ. 2014.
69. T. Christen and M. W. Carlen, *J. Power Sources*, **91**, No. 2, 210-216 (2000), doi: 10.1016/S0378-7753(00)00474-2.
70. D. V. Ragone, *Society of Automotive Engineers. Mid-year Meeting*, Detroit, Michigan, May 20-24, SAE International, New York (1968), Art. 680453.
71. H. Budde-Meiwes, J. Drillkens, et al., *P. I. Mech. Eng. D-J. Aut.*, **227**, No. 5, 761-776 (2013), doi: 10.1177/0954407013485567.
72. B. E. Paton, A. M. Zhikharev, D. M. Kaleko, and O. O. Slezin, *Stud Welding Machine* [in Ukrainian], Patent Ukraine No. 100828, Publ. 25.01.2013.